热带亚热带植物学报 2016, 24(2): 128 ~ 142
Journal of Tropical and Subtropical Botany

*de novo*转录组学分析华南地区入侵植物五爪金龙代谢特征

耿妍[1], 陈玲玲[1], 鲁焕[1], 宁婵娟[1], BJÖRN Lars Olof[1,2], 李韶山[1*]
(1. 华南师范大学生命科学学院，广东省高校生态学与环境科学重点实验室，广州 510631; 2. 隆德大学生物学系，隆德 SE-22362, 瑞典)

摘要：为探究华南地区严重入侵植物五爪金龙(*Ipomoea cairica*)生物入侵的分子机制，对五爪金龙及其近缘种七爪金龙(*I. digitata*)和裂叶牵牛(*I. nil*)进行 *de novo* 转录组测序和组装，得到 56551 条 unigenes，其中 56522 条得到注释，7815 条 GO 注释，15615 条 COG 注释，180201 条 KEGG 数据库注释。转录组分析结果表明，五爪金龙氮代谢通路关键酶基因的表达高于对照。次生代谢关键酶(PAL、4CL、CAD、查耳酮合酶、苯基丙乙烯酮异构酶、槲皮黄 3-*O*-甲基转移酶等)基因在五爪金龙与七爪金龙及裂叶牵牛中均得到协同性的差异表达，而这些代谢通路指导的产物合成对五爪金龙的抗逆境能力、生长、化感作用等均起关键作用。关键基因的 RT-qPCR 验证结果与转录组结果具有一致性。因此，这从分子生物学层面上对解释五爪金龙在华南地区的入侵机制提供了新的证据。

关键词：*de novo*；转录组；五爪金龙；生物入侵；代谢
doi: 10.11926/j.issn.1005−3395.2016.02.002

Metabolic Characteristics of Invasive Plant *Ipomoea cairica* in South China by *de novo* Transcriptomics

GENG Yan[1], CHEN Ling-ling[1], LU Huan[1], NING Chan-juan[1], BJÖRN Lars Olof[1,2], LI Shao-shan[1*]
(1. *School of Life Science, Key Laboratory of Ecology and Environmental Science in Guangdong Higher Education, South China Normal University*, Guangzhou 510631, China; 2. *Department of Biology, Lund University*, Sölvegatan 35, SE-223 62 Lund, Sweden)

Abstract: To explore the molecular mechanisms of *Ipomoea cairica* invasiveness in south China, the *de novo* transcriptomes from *I. cairica* and two related species, *I. digitata* and *I. nil*, were sequenced and assembled. There were 56551 all-unigenes obtained by assembling the reads, among them 56522 all-unigenes were annotated, including 7815, 15615, and 180201 all-unigenes in GO, COG and KEGG databases, respectively. Moreover, the activities of NR and GS in *I. cairica*, key enzyme in metabolic pathway for nitrogen, were greater than those in related species. In addition, the transcriptome data showed that the genes of key enzymes in secondary metabolism, such as *pal, 4cl, cad, chs*, and *chi*, had synergic differential expression in *I. cairica*, *I. digitata* and *I. nil*. The production synthesis from metabolic pathway could play a key role in stress-resistant, growth and allelopathy of *I. cairica*. The RT-qPCR verification results of key genes were similar to those from transcriptome. Therefore, the result of the present research might explain partly the successful invasiveness of *I. cairica* in South China at the level of molecular biology.

Key words: *de novo*; Transcriptome; RNA-seq; *Ipomoea cairica*; Biological invasion; Metabolism

Received: 2015–06–29 **Accepted:** 2015–09–25
This work was supported by the Natural Science Foundation of China (Grant No. 31070242), the Research Fund for the Doctoral Program, Ministry of Education, China (Grant No. 20114407110006), the Leading Scientists Project of Pearl River Scholar Fund in Guangdong Province (Grant No. 2012).
GENG Yan, female, MD, interested in comparative transcriptomics and bioinformatics analysis of invasive plants. E-mail: gengyan_xx@163.com
* Corresponding author. E-mail: lishsh@scnu.edu.cn

Ipomoea cairica (Convolvulaceae) is a perennial herb with trumpet-shaped flowers and five-lobed leaf blades[1]. It was planted as an ornamental plant at first, but later became invasive. It originated in South or Central America, naturalized in Hong Kong in 1921, and is widespread in southern China[2]. The plant grows in full sun with well-drained soil, such as flat ground, road side and brush with sufficient sunlight. Unfortunately, it grows not only along the ground but also climbs and covers other plants. The covered plants are damaged and even die because of reducing sunlight[3]. Due to its rapid growth, strong environmental adaptability, and high photosynthetic capacity, *I. cairica* has rapidly spread in tropical and subtropical regions and has become one of the most severe alien invasive plants in south China. Thus, this invasive species markedly reduces biodiversity and damages the landscapes of gardens, becoming one of the most detrimental weeds in southern China[4], second only to *Mikania micrantha* Kunth. *Ipomoea digitata*, an annual weed, with flowers similar to *I. cairica* but 5−7-lobed leaf blades, is a non-invasive species growing in south China. *Ipomoea nil*, an annual weed with 3-lobed leaf blades, has become widespread in southern China and listed as a mildly invasive plant.

There are several protein sequences for *Ipomoea* available in GenBank, but as the total number of DNA and mRNA sequences is limited, we investigated the transcriptome of *I. cairica*, setting *I. nil* and *I. digitata* as controls, using next-generation sequencing technology with *de novo* transcriptome assembly. The assembled, annotated transcriptome sequences will provide a valuable genomic resource for further understanding the molecular basis of plant invasion as well as for conducting additional studies.

Many reports from Brazil, Japan[5], Malaysia[6] and China (Hong Kong)[7] have mentioned the use of *I. cairica* in folk medicine. Most studies on *I. cairica* focused on biochemical[1,8] and ecological characteristics[3], but its genome and transcriptome has seldom been reported. Shekhar et al.[9] conducted a differential transcript expression analysis, but only between two cultivars of *I. batatas*. The allelopathy of *I. cairica* inhibiting seed germination has been reported, but the secondary metabolism of *I. cairica* that produces chemical weapons and the molecular mechanisms of this meta- bolism have not been studied. Two factors limiting further study are the lack of physiological comparisons between the original species in South America and the native species in China, and not understanding the reasons that *I. cairica* is invasive in southern China.

Nitrogen, an essential element for plant growth and development, is one of the important indicators of resource capture capabilities in invasive plants. Therefore, this study explored the nitrogen capture capabilities of *I. cairica* by comparing this process in *I. cairica* to that in related species, *I. digitata* (native to southern China) and *I. nil* (mildly invasive), belonging to Convolvulaceae.

1 Materials and methods

1.1 Sample preparation and assembly

Samples of *I. cairica*, *I. digitata*, and *I. nil* were collected from South China Normal University (Guangzhou, Guangdong, south China) in September, 2011 in a phase of rapid growth. Samples had the same growth vigour, young stem tips with a length from 10 cm to 15 cm were used in this study.

The total RNA extraction was conducted using a polysaccharide and polyphenol-free RNA extraction kit (BioTeke, Catalog number RP3201). The RNA was enriched using magnetic beads with Oligo(dT) fragmented into short segments using fragmentation buffer. Based on mRNA templates, the first-strand cDNA synthesis was conducted with random hexamers, and then buffer, dNTPs, RNase H and DNA polymerase I was introduced for the synthesis of the second cDNA strand. The products were purified using a QiaQuick PCR kit and eluted with EB buffer. The ends were repaired and the sequencing joints connected. The fragments were detected using agarose gel electrophoresis followed by PCR. The cDNA library was sequenced using an Illumina HiSeq 2000 instrument.

Bioinformatics analyses were applied to the

sequencing results. The original image data were transformed into sequence data using base calling. Before assembly, adaptor sequences, meaning reads containing more than 10% 'N' (where N represents ambiguous bases in reads), and low quality sequences (reads in which more than 50% of the bases had a quality value<10) were removed. The 90 bp raw reads were then filtered to obtain high-quality clean reads.

The short-sequencing reads were assembled using SOAP *de novo* software[10]. SOAP *de novo* first connected reads of significant overlap into longer fragments and then obtained contigs without unknown sequences (N) between two contigs. The reads were re-compared with the contigs, ensuring different contigs from the same transcripts and the distance of these contigs using paired-end reads. SOAP *de novo* connected these contigs, with the unknown sequences (N) in the middle, and then obtained the scaffolds. The gaps in the scaffolds were filled using paired-end reads, obtaining unigenes with the least N that could not be extended at both ends. The unigenes from different samples were further assembled with redundancies eliminated to obtain the longest possible unigenes with no redundancies.

Finally, BLASTx alignment (https://blast.ncbi.nlm.nih.gov/Blast.cgi?PROGRAM=blastx&PAGE_TYPE=BlastSearch&BLAST_SPEC=blast2seq&LINK_LOC=blasttab) was conducted to compare the unigene sequences to several protein databases, including non-redundant (nr) NCBI, Swiss-Prot, Kyoto Encyclopedia of Genes and Genomes (KEGG), and Cluster of Orthologous Groups (COG). BLAST matches with E-value scores less than 0.00001 were considered significant. The resulting best score for the alignment was used to determine the sequence direction. If contradictions occurred in the results from the different databases, then the orientation of the unigenes were determined following the priority scheme of nr, followed by Swiss-Prot, KEGG, and finally COG. If the unigenes were not comparable with any of these protein databases, then the coding region was predicted and the orient of the sequence was determined using ESTScan[11–12]. For unigenes with sequence direction, we provided their sequences from the 5′ end to 3′ end, for those without any direction, we provided their sequences from assembly software.

1.2 Functional annotation

The unigenes were functionally annotated. The BLAST search for the unigenes was run against the COG database of proteins to predict the functional categories and classification statistics, obtaining the gene functional characteristics at the macro level.

The nr annotated unigenes were mapped against the Gene Ontology (GO) database to retrieve functional annotations through GO terms. A statistical analysis of the GO terms offered the functional characteristics of the genes at the macro level. After obtaining the GO classifications, the unigenes were mapped to the KEGG database to determine functional annotations and generate corresponding pathway maps for the unigenes[13], providing relationship information for the unigenes, the species and their interactions with the environment.

1.3 Predictive coding protein box

The sequence was translated into its amino acid sequence using a standard code table, and the nucleotide sequence was obtained. If none of the above databases were successfully blasted against the unigene, then the coding region was predicted to determine the orientation of the nucleotide sequence (5′ to 3′) and amino acid sequence using EST Scan[11].

1.4 Differentially expressed genes

Differential gene expression analysis was conducted according to the method of Audic, et al[14]. The distribution of $P(x)$ follows a Poisson distribution (Eq. 1), λ is the number of real transcripts.

$$P(x)=\frac{e^{-\lambda}\lambda^{x}}{x!} \quad \text{(Eq. 1)}$$

The probability that the expression of gene A is equal in both samples is calculated using Eq. 2[14].

$$P(y\mid X)=\left(\frac{N_2}{N_1}\right)^{y}\frac{(x+y)!}{x!y!\left(1+\frac{N_2}{N_1}\right)^{(x+y+1)}}$$

$$2\sum_{i=0}^{i=y}p(i\mid x) \text{ or } 2\left(1-\sum_{i=0}^{i=y}p(i\mid x)\right) \text{ if } \sum_{i=0}^{i=y}p(i\mid x)>0.5 \quad \text{(Eq. 2)}$$

The differences in the P-values for multiple hypothesis testing were examined, and the thresholds of

the P-values were decided using the false discovery rate (FDR) method[15]. After this analysis was conducted, the GO function and KEGG pathway were analyzed.

The expression of the unigene was calculated using the RPKM method[16] (Eq. 3). It can determine the effect of gene length and sequencing differences on gene expression and can be used to directly compare different samples.

$$\mathrm{RPKM} = \frac{10^6 \mathrm{G}}{(NL)/10^3} \quad \text{(Eq. 3)}$$

When RPKM(A) is assumed to be the expression of unigene A, then C denotes the number of reads blasted to only unigene A, *N* denotes the total number of reads which could be blasted to all unigenes, and *L* denotes the number of bases in unigene A.

1.5 GO and pathway analysis of differentially expressed genes

The GO analysis[17] of differential gene expression provides molecular function, biological process and cellular component annotations, and can also determine significantly enriched functions in the differentially expressed genes. All of the differentially expressed genes were first mapped onto the average terms in the GO database (http://www.geneontology.org/). The number of genes in every term was calculated and the significantly enriched genes were determined by comparing the genome with a super geometry inspection according to Eq. 4.

$$P = \sum_{i=0}^{m-1} \frac{\binom{M}{i}\binom{N-M}{n-i}}{\binom{N}{n}} \quad \text{(Eq. 4)}$$

N denotes the number of genes annotated by GO, *n* denotes the number of differentially expressed genes, and *M* denotes the number of genes annotated with the special GO terms in all unigenes.

Thus, the main biological functions of the differentially expressed genes were determined using GO enrichment analysis[17].

1.6 Confirmation using Real-time qPCR

Primers were designed using Primer 3.0. The primer sequence and gene characteristics are summarized in Table 1.

The RT-PCR reactions were performed using an Applied Biosystems 7500 Real-time PCR system with SYBR Premix Taq (TaKaRa) in 96 connected tubes (TaKaRa). Each sample was analyzed in triplicate in a 20 μL reaction volume, containing 0.5 μL of each primer, 10 μL of SYBR Green I, 1 μL of diluted cDNA, and 8 μL of RNase free dH_2O. For each experiment, the endogenous control gene actin was analyzed in triplicate (positive control) with a non-template reaction (negative control) and a water only reaction (blank control). The relative expression levels were calculated using the $2^{-\Delta\Delta C_T}$ method[18].

Table 1 Nucleotide sequences of the primers used in SYBR Green I RT-qPCR

Gene	Species	Primer sequences (5′~3′)
Actin	*I. cairica*	GCGGATAGAATGAGCAAGGAA
		GGGCCGGACTCATCATACTC
	I. digitata	TTGTAGCACCACCTGAAAGGAAAT
		CGGACTCATCATACTCTGCCTTG
	I. nil	TGTGACAATGGAACTGGAATGGT
		TTGATTGAGCTTCATCTCCGACAT
Nitrate reductase	*I. cairica*	TCACTCGAGGTCGAGGTTC
		CTCGAGGTGTCTTTCCTTC
	I. digitata	CCTTCATGAACACGGCTTCT
		TTCTTCGCCTTATCGGAGTG
	I. nil	TCTTCATCTGCGCCGCCATTG
		GGGAGTCGAGGTGTTGGGACAT
Glutamine synthetase	*I. cairica*	CTCCAGCAGGTGAGCCTATC
		AGCCTTGTCTGCACCAATTC
	I. digitata	TGAGGAGCAAAGCCAGGACCAT
		ACTGTCCTCTCCAGGAGCTTGG
	I. nil	CGGGAGAGGACAGTGAAGTC
		ACCAAGTGGCCATTTCACAT

1.7 Determination of total nitrogen content of leaf (TN)

TN in leaf was determined by using sulfuric acid-hydrogen peroxide digestion-distillation and titration method[19].

1.8 Determination of activities of NR and GS

The activity of NR (NRA) was determined by using colorimetric determination of sulfanilamide *in vivo*[20].

The activity of GS (GSA) was determined in the following way: (1) From leaves, young stems and roots of each species 0.2 g samples were collected; (2) Three mL ice-cold extraction buffer [50 mmol L^{-1} Tris-HCl (pH 7.5), 10 mmol L^{-1} $MgCl_2$, 1 mmol L^{-1} EDTA, 10% (w/v) glycerol, 14 mmol L^{-1} mercap-

toethanol] and 1% (w/v) PVP] was added, then ground on ice until homogenized; (3) The homogenate was put into 1.5 mL microtubes, and centrifuged for 30 min at 4℃, 13000×*g*. Then the enzyme extracts were transferred to new centrifuge tubes for standby. For the next steps the GS testing kit directions of Nanjing Jiancheng Bioengineering Institute were followed.

2 Results and discussion

2.1 Sequencing and assembly

There were 26501994, 26901752 and 23139614 high-quality reads obtained from *I. cairica*, *I. digitata* and *I. nil*, respectively, and assembled them using SOAP *de novo* to obtain 384401 contigs with a mean length of 164 nt in *I. cairica*, 352302 contigs with a mean length of 171 bp in *I. digitata*, and 368222 contigs with a mean length of 157 bp in *I. nil* (Table 2). With paired-end read joining and gap-filling, the above contigs were further assembled into 124007 scaffolds with a mean size of 343 bp in *I. cairica*, 112882 scaffolds with a mean size of 342 bp in *I. digitata*, and 98903 scaffolds with a mean size of 362 bp in *I. nil*. Using gap filling and long sequence clustering, the scaffolds were assembled into 90329 *I. cairica* unigenes with a mean length of 423 bp, 86946 *I. digitata* unigenes with a mean length of 441 bp, and 77255 *I. nil* unigenes with a mean length of 428 bp. In addition, using the same strategy, we obtained 56551 all-unigenes with a mean length of 781 bp from the *I. cairica*, *I. digitata* and *I. nil* reads combined (all-unigenes originated from all of the *I. cairica*, *I. digitata* and *I. nil* reads, and unigenes of each species from itself reads).

Table 2 Transcriptome qualities in *Ipomoea cairica*, *I. digitata*, and *I. nil*

	I. cairica	*I. digitata*	*I. nil*	Total
Total nucleotides (nt)	2385179460	2421157680	2082565260	–
Total number of reads	26501994	26901752	23139614	–
GC content (%)	47.75	47.79	48.66	–
Total number of contigs	384401	352302	368222	–
Mean length of contigs (bp)	164	171	157	–
Total number of scaffolds	124007	112882	98903	–
Mean length of scaffolds (bp)	343	369	362	–
The number of unigenes	90329	86946	77255	–
Mean length of unigenes	423	441	428	–
Number of all-unigenes	–	–	–	56551
Mean length of all-unigenes	–	–	–	781

For reads, the original data were transformed into sequence data by base calling from raw data or raw reads obtained as clean reads after removal of impurities. For contigs, joint reads with overlap into longer fragments without unknown sequences between each two contigs (N) using SOAP *de novo* software. For scaffolds, contigs joined using SOAP *de novo* software. Unigenes represent sequences that cannot be extended on either end and contain the least N.

The length and gap distributions of unigenes from three species and all-unigene are shown in Fig. 1. Overall, all-unigenes were better in quality than unigenes from one of three species and obtained higher scores when using BLASTx to search against the nr database.

2.2 GO and COG classifications

We further classified all-unigenes using GO assignments after functional annotation. Based on homologous genes, 37815 all-unigenes were categorized into 44 GO terms under three domains: biological process, cellular component and molecular function (Fig. 2). The results indicated that the terms with the highest percentage were cell, cell part, cell process and metabolic process, whereas no genes were assigned to the terms biology adhesion, cell killing, location, viral reproduction, viron, viron part or electron activity. To further examine the integrity of our transcriptome library and effectiveness of the annotation process, we calculated the unigene numbers with COG classifications. There were 15615 all-unigenes with a COG classification (Fig. 3).

Of the 25 COG categories, the cluster predicting general function had the highest number of unigenes, followed by that for transcription, whereas the clusters of nuclear structure and extracellular structure had the fewest number of unigenes (Fig. 3).

GO categories, shown on the X-axis, are group into three ontologies: biological process, cellular component, and molecular function. The right Y-axis indicates the number of genes in each category, and the left Y-axis indicates the percentage of total genes in that category. 'All-unigene' indicates that the unigenes were assembled from reads of *I. cairica, I. digitata* and *I. nil* samples.

15615 unigenes were assigned to 25 categories in the COG functional classification. The Y-axis indicates the number of genes in a specific functional cluster. The legend to the right of the histogram lists the 25 functional categories.

2.3 Unigene networks and differentially expressed gene pathway enrichment analysis

The biological pathways in *I. cairica, I. digitata* and *I. nil* were analyzed. There were 25725 all-unigenes mapped to Nr database, 30832 all-unigenes mapped to Swiss-Prot database, 23659 all-unigenes mapped to the KEGG database, 15615 mapped to COG database and 37815 mapped to GO. In a more detailed analysis, frequency of 30020 all-unigenes assigned to 119 different pathways (Data not show). To identify gene expression without taking into account the effects of different gene lengths or differences in the total number of reads, we used the transformed RPKM value with a false discovery rate (FDR)$\leqslant$0.001 and a $\log_2$ ratio$\geqslant$1 (representing at least a 2-fold change) to signify differences in gene expression. We use these assumptions to analyze the differences between *I. cairica* vs *I. digitata*, *I. cairica* vs *I. nil*, and *I. digitata* vs *I. nil*.

2.4 Total leaf nitrogen content

The total nitrogen (TN) content represents an important physiological indicator of nitrogen use efficiency in plants. In present experiment, it is found that TN in *I. cairica* was significantly higher than that in the related species (Fig. 4).

2.5 Nitrate reductase and glutamine synthetase activities

The activity of nitrate reductase (NR), involved in the first and rate-limiting step for the NO_3^- assimilation process, directly affects the efficiency of NO_3^- assimilation. The NR activity in leaf, stem, and root was significantly higher in *I. cairica* than that in two related species (Fig. 5: A).

Glutamine synthetase (GS) is a multifunctional enzyme involved in the regulation a variety of processes in nitrogen metabolism. GS activity can reflect the capacity of nitrogen assimilation[21]. The GS activity in stem was significantly higher in *I. cairica* than that in two related species (Fig. 5: B).

2.6 Differential gene expression in nitrogen metabolism

A comparison of the expression of genes involved in the nitrogen pathway in *I. cairica* vs. *I. digitata* and in *I. cairica* vs. *I. nil* demonstrated some DEGs (FDR$\leqslant$0.001 and $\log_2$ ratio$\geqslant$1). A total of 84 DEGs were detected between *I. cairica* and *I. digitata*, in which 48 unigenes were up-regulated and 36 unigenes were down-regulated. Similarly, a totalof 79 DEGs were detected between *I. cairica* and *I. nil*, in which 52 unigenes were up-regulated and 27 unigenes were down-regulated.

Before undertaking an analysis of the differences in transcript abundance among the three species, we used real-time quantitative PCR to confirm the estimates of transcript abundance obtained with RNA-seq. We chose to examine genes encoding NR and GS. The results showed that the gene expression profiles obtained with the two methods were similar (Fig. 6). Therefore, the ratios of transcript abundance obtained using RNA-seq are suitable for calling DEGs between *I. cairica* and its two related species.

2.7 Functional annotation analysis of DEGs in nitrogen metabolism

To further understand the function of co-DEGs, we mapped them using the KEGG database for analysis of nitrogen metabolism pathway (Table 4). DEGs code for important enzymes in nitrogen metabolism, for example, NR and GS. In addition, the levels of most of co-DEGs were up-regulated in *I. cairica* compared

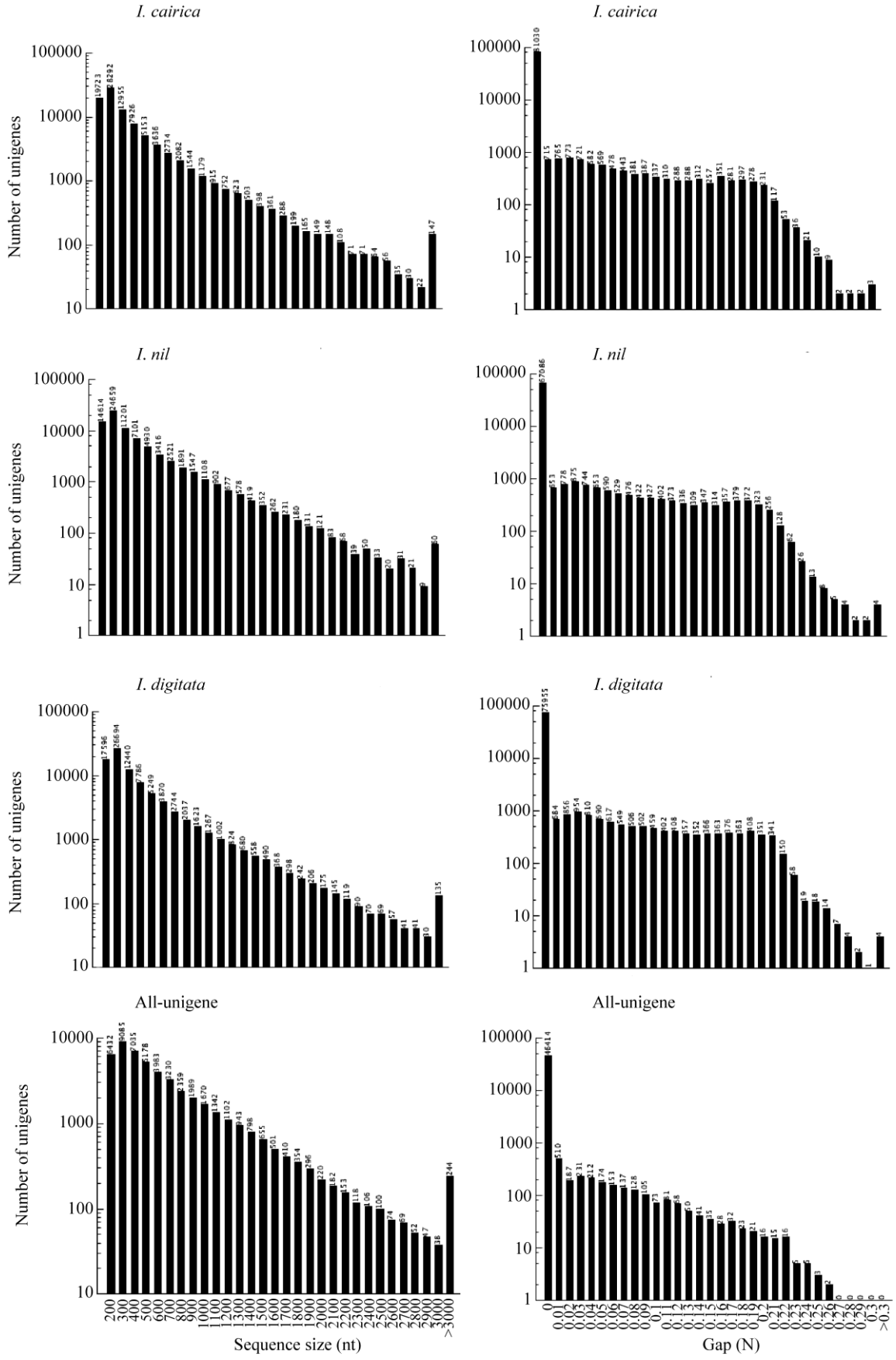

Fig. 1 Length and gap distributions of unigenes after *de novo* assembly using the reads from *Ipomoea cairica*, *I. digitata*, *I. nil* and all samples.

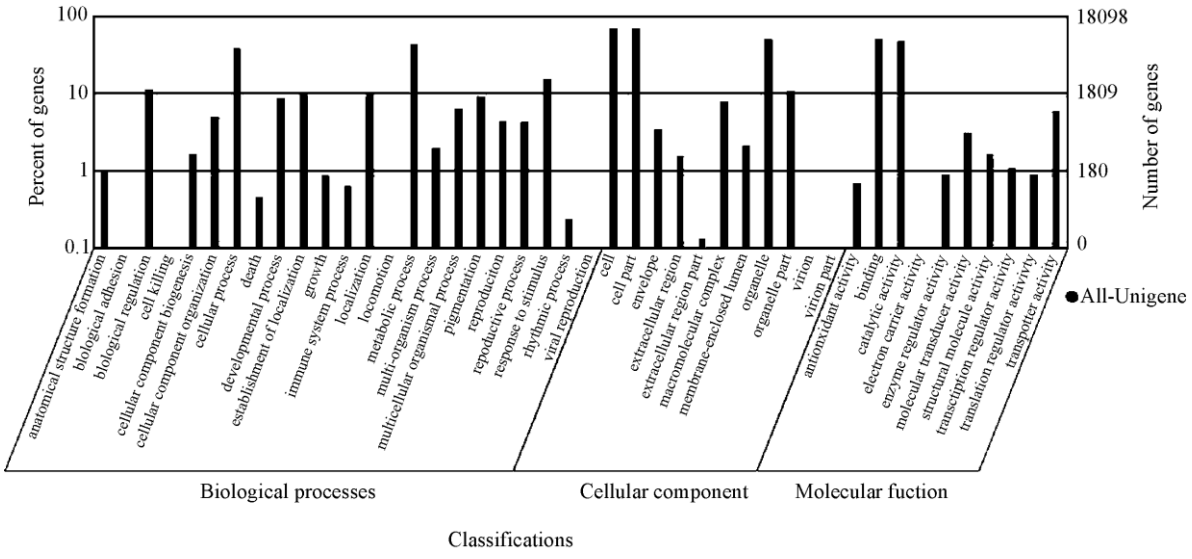

Fig. 2 Histogram of gene ontology classification

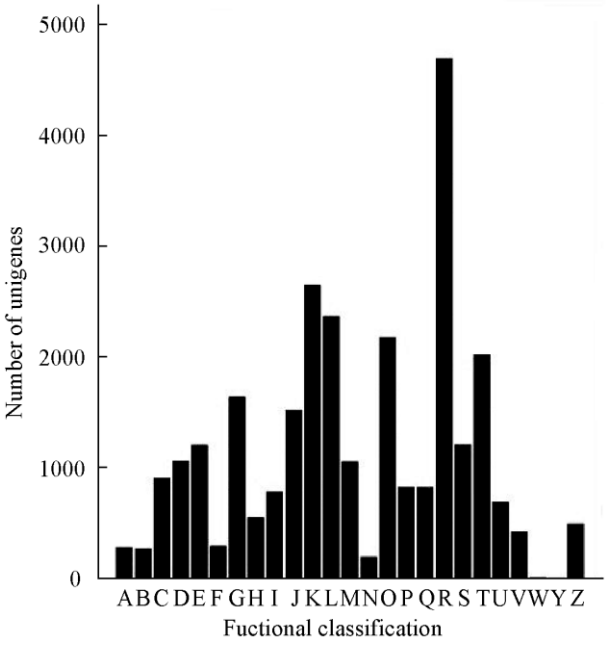

Fig. 3 Histogram of clusters of orthologous groups (COG) classification. A: RNA processing and modification; B: Chromatin structure and dynamics; C: Energy production and conversion; D: Cell cycle control, cell division, chromosome partitioning; E: Amino acid transport and metabolism; F: Nucleotide transport and metabolism; G: Carbohydrate transport and metabolism; H: Coenzyme transport and metabolism; I: Lipd transport and metabolism; J: Translation, ribosomal structure and biogensis, K: Transcription, L: Replication, recombination and repair; M: Cell wall/membrane/envelope biogenesis; N: Cell motility; O: Posttranslational modification, protein turnover, chaperones; P: Inorganic ion transport and metabolism; Q: Secondary metabolites biosynthesis, transport and catabolism; R: General function prediction only; S: Function unkown; T: Signal transduction mechanism; U: Intracellular trafficking, secretion, and vesicular transport; V: Defense mechanism; W: Extracellular structures; Y: Nuclear structures; Z: Cytoskeleton.

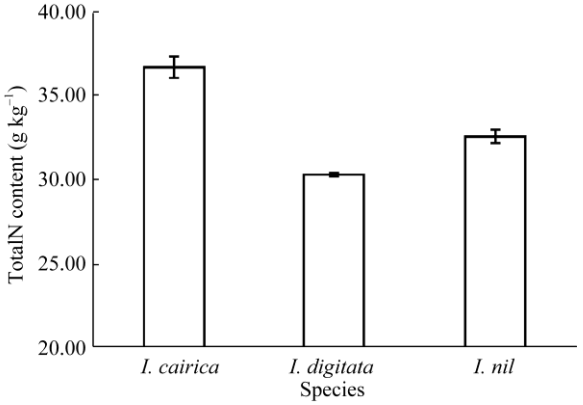

Fig. 4 Total nitrogen content in leaves

with those in other two species.

2.8 Transcripts related to secondary metabolism in biosynthetic pathways

We also examine pathways related to the biosynthesis of secondary metabolites, specifically the biosynthesis of phenylpropanoid (KO00940), flavonoid (KO00944), and flavones and flavonol (KO00941). The results of the statistical analyses revealed that for phenylpropanoid biosynthesis (KO00940) there were 333 differentially expressed unigenes between *I. cairica* and *I. digitata*, as well as 348 between *I. cairica* and *I. nil*; there were 220 unigenes differentially expressed for *I. cairica* compared with both *I. digitata* and *I. nil*. For flavonoid biosynthesis (KO00944), there were 205, 208 and 139 differentially expressed unigenes, and for flavones and flavonol biosynthesis (KO00941)

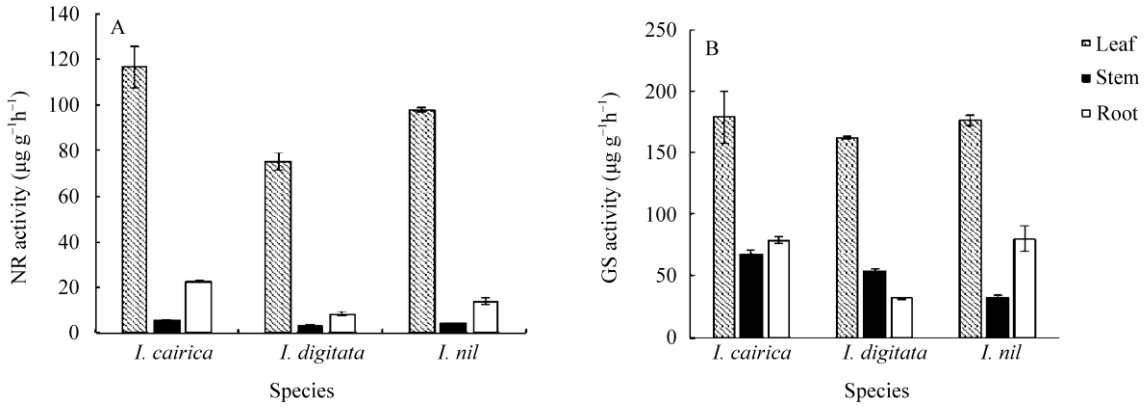

Fig. 5 Nitrate reductase (NR) (A) glutamine synthetase (GS) (B) activity in leaves, stems and roots of *Ipomoea cairica*, *I. digitata*, and *I. nil*

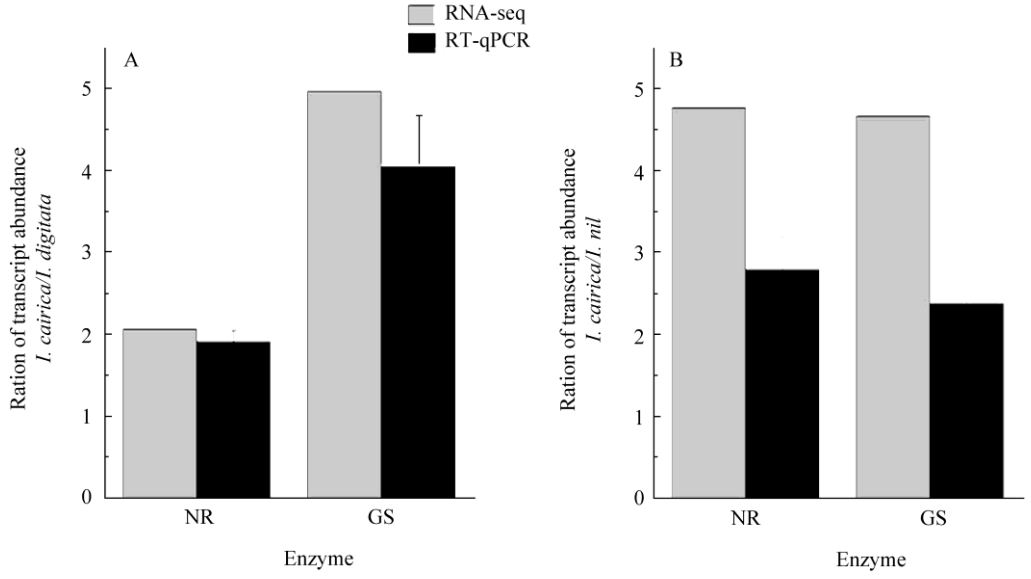

Fig. 6 RT-PCR detection and RNA sequencing in *Ipomoea cairica* vs *I. digitata* (A) and *I. cairica* vs *I. nil* (B)

there were 59, 51 and 33 differentially expressed unigenes, and for the biosynthesis of the secondary metabolites with COGs there were 1398, 1446, and 926 between *I. cairica* and *I. digitata*, between *I. cairica* and *I. nil*, and for both *I. digitata* and *I. nil*, respectively. Taken together, these data indicated the existence of duplicate genes. Therefore, we removed the duplicates and obtained 964 unigenes, with *I. cairica* different from both *I. digitata* and *I. nil* (Data not show). Among all those differences, between *I. cairica* and *I. digitata*, *I. cairica* and *I. nil*, there were 493 unigenes up-regulated and 303 unigenes down-regulated. These results indicated that the differences were comparable for both models, with 706 similarly expressed genes, which was 82.57% of the total. Those differentially expressed genes may explain the differences in the biosynthesis of these secondary metabolites in *I. cairica* compared with that in *I. digitata* and *I. nil*. It would be interesting to determine whether those differences were related to the invasiveness of *I. cairica.*

After further analysis of the annotations for those differential genes, we found up-regulated expression of some genes, Unigene32623_All, Unigene19708_ All and Unigene32546_All code *pal2*, 33181_All code *pal4*, related to a key enzyme in the biosynthesis of secondary metabolites, phenylalanine ammonia lyase (PAL), and the down-regulation of another PAL-related gene, unigene4820_All code *pal6*, in *I. cairica*.

2.9 Analysis of physiological indexes

This study used high-throughput and *de novo* transcriptome assembly methods to provide trans-

criptome information for three species of *Ipomoea*, three non-model plants. However, the invasion of *I. cairica* is complex, with allelopathy and stress-resistance both necessary and contributing to its success. Previous studies have reported on the allelochemicals and stress-resistance in *I. cairica*.

Our results indicated that the TN content in the leaves of *I. cairica* was markedly higher than that in the two related plants. However, this result did not discriminate whether *I. cairica* had a greater capacity for nitrogen absorption, reduction, or fixation. Nitrate reductase is the first key enzyme in the nitrogen metabolism pathway and is widely found in roots, stems, leaves, and other tissues of higher plants. Evidence indicates that the activity of NR reflects the status of nitrogen nutrition and nitrogen metabolism in plants as well as directly impacts the efficiency of inorganic nitrogen use from soil and the synthesis rate of amino acids in plants[22]. NO is an intracellular and extracellular signaling molecule involved in various processes that promote plant growth and development and alleviate aging and stress damage[23]. Glutamine synthetase, another key enzyme in the nitrogen metabolism pathway, plays an important role in ammonia assimilation. Data indicate that GS activity enhances ammonium assimilation and nitrogen transformation[24]. In the present study, NR activity was markedly higher in the roots, stems and leaves and GS activity was significantly higher in the stems of *I. cairica* compared with those in the two related species (Fig. 5). Studies have shown that increased nutrient availability favors the invasion and success of invasive plant species in ecosystems where resource availability is typically low[25]. Nitrogen is the most important nutrient limiting plant growth and development. Studying nitrogen utilization benefits understanding of nutrient adaptation mechanisms in invasive species[26]. The nitrogen assimilation capacity of *I. cairica* is greater than that of the native plant *Paederia scandens*[27]. Our results showed that NR and GS activity as well as TN content in the leaves of *I. cairica* were superior to those in the two related species. Thus, the enahnced ability of *I. cairica* to metabolize nitrogen and accelerate nitrogen transformation is likely an important mechanism in its successful invasion.

2.10 Analysis of DEGs in the nitrogen metabolic pathway

To better understand the biological functions of DEGs in nitrogen metabolism, we used the KEGG database to analyze the nitrogen metabolism pathway (KO00910). In this experiment, 39 co-DEGs were identified and annotated for *I. cairica* and its two related species (Table 3). Interestingly, most of the co-DEGs were up-regulated, suggesting they may play an important role in capturing nitrogen resources for *I. cairica.*

It is generally believed that nitrate is the main form of nitrogen absorbed by plants. Nitrate reductase is the enzyme used in the first step for catalyzing nitrate assimilation, and its synthesis is strictly modulated at the transcriptional and post-transcriptional levels[28]. It was reported that the double mutant *Arabidopsis* NR (*nia1*, *nia2*) is etiolated, the content of leaf amino acid is reduced, and it grows more slowly compared with the wild type[29]. Nitrite reductase (NiR) is involved in the second step for nitrate assimilation, which catalyzes the reduction of nitrite to ammonium. The higher activity of NiR prevents toxic effects by accumulating NO_2 on plants, and provides ammonia for assimilation in next step[30]. The overexpression of *NR* or *NiR* enhances mRNA levels, and improves nitrogen assimilation in plants[31]. Transcriptomics analysis in the present study showed differential regulation for *NR* and *NiR* gene expression, with expression up-regulated in *I. cairica* relative to the other two species, indicating that the invasive *I. cairica* has a stronger ability to assimilate nitrate.

Ammonia is assimilated in plants by the glutamine synthetase/glutamate synthase (GS/GOGAT) cycle or glutamate dehydrogenase (GDH) pathway[32]. The GS/GOGAT cycle is the major pathway for ammonia assimilation in higher plants, whereas the key enzyme GS plays a central role in nitrogen metabolism of

Table 3 Annotation of differentially expressed unigenes in nitrogen metabolism in *Ipomoea cairica* (IC) vs. *I. digitata* (ID) and in *I. cairica* vs. *I. nil* (IN)

Gene ID	*IC* vs. *ID*	*IC* vs. *IN*	Annotation	Gene name [species]	Database
Unigene24221_All	13.7	1.4	Probable cytochrome b5 isoform 2	NR [Vf]	KEGG
Unigene25910_All	12.6	12.6	Delta(5) fatty acid desaturase B	NR [Nt]	KEGG
Unigene10704_All	5.2	1.8	Ferredoxin-nitrite reductase	ferredoxin-NiR [Nt]	KEGG
Unigene27753_All	2.8	14.5	Laccase-12	NiR (NO-forming) [Gm]	KEGG
Unigene38636_All	1.9	4.3	Laccase-17	NiR (NO-forming) [Pt]	KEGG
Unigene14693_All	–2.9	13.2	Glutamate synthase [NADH]	GS [Vv]	KEGG
Unigene31766_All	3.5	14.3	Glutamine synthetase leaf isozyme	GS [Cl]	KEGG
Unigene15163_All	5.0	4.7	Glutamine synthetase nodule isozyme	GS [Hb]	KEGG
Unigene31658_All	1.3	3.3	Glutamine synthetase root isozyme B	GS [Eu]	KEGG
Unigene18636_All	4.3	12.6	Glutamate dehydrogenase A	GDH(NAD(P)+) [Np]	KEGG
Unigene27731_All	5.4	4.2	Glutamate dehydrogenase A	GDH(NAD(P)+) [Np]	KEGG
Unigene9230_All	1.9	1.5	Glutamate dehydrogenase A	GDH(NAD(P)+) [Np]	KEGG
Unigene35570_All	1.6	1.4	Glutamate dehydrogenase A	GDH(NAD(P)+) [Np]	KEGG
Unigene31232_All	4.4	5.0	Probable glutamate dehydrogenase 3	GDH(NAD(P)+) [At]	KEGG
Unigene49856_All	3.1	1.4	Glutamate dehydrogenase	GDH(NAD(P)+) [Ac]	KEGG
Unigene25819_All	3.7	8.4	Asparagine synthetase, nodule	AS [Sp]	KEGG
Unigene11157_All	2.5	4.3	Asparagine synthetase	AS [Ha]	KEGG
Unigene33181_All	17.4	17.4	Phenylalanine ammonia-lyase 1	PAL [Cc]	KEGG
Unigene32546_All	3.7	17.4	Phenylalanine ammonia-lyase	PAL [Me]	KEGG
Unigene32623_All	1.9	2.1	Phenylalanine ammonia-lyase	PAL [Ib]	KEGG
Unigene19708_All	1.8	1.5	Phenylalanine ammonia-lyase	PAL [Ib]	KEGG
Unigene32744_All	2.2	2.8	Laccase-2	L-ascorbate oxidases [Pt]	KEGG
Unigene31161_All	7.1	4.7	Laccase-3	L-ascorbate oxidase [At]	KEGG
Unigene31213_All	12.4	12.4	Laccase-4	L-ascorbate oxidase [Pt]	KEGG
Unigene26200_All	4.5	4.9	Laccase-6	L-ascorbate oxidase [At]	KEGG
Unigene25388_All	8.1	13.8	Laccase-11	L-ascorbate oxidase [At]	KEGG
Unigene26384_All	3.6	3.9	Laccase-12	L-ascorbate oxidase [At]	KEGG
Unigene16438_All	1.1	1.0	Laccase-12	L-ascorbate oxidase [Pt]	KEGG
Unigene19574_All	1.6	2.0	Laccase-17	L-ascorbate oxidase [Lt]	KEGG
Unigene34362_All	2.3	10.2	L-ascorbate oxidase homolog	L-ascorbate oxidase [Nt]	KEGG
Unigene32435_All	5.4	4.0	L-ascorbate oxidase	L-ascorbate oxidase [Nt]	KEGG
Unigene10363_All	–1.9	–1.5	L-ascorbate oxidase homolog	L-ascorbate oxidase [Mt]	KEGG
Unigene12570_All	–1.0	–1.6	L-ascorbate oxidase homolog	L-ascorbate oxidase [Nt]	KEGG
Unigene147_All	–2.3	–4.8	Laccase-4	L-ascorbate oxidase [Nt]	KEGG
Unigene13298_All	–4.6	–6.5	Phosphopantetheineadenylyltransferase	L-ascorbate oxidase [At]	KEGG
Unigene31031_All	13.2	4.1	Flavin-containing monooxygenase FMOGS-OX5	Dimethylaniline monooxygenase [Alsl]	KEGG
Unigene21078_All	1.1	2.4	Carbonic anhydrase	Carbonic anhydrase [Alsl]	KEGG
Unigene21626_All	1.4	1.6	Cyanatehydratase	Cyanatelyase [Zm]	KEGG
Unigene30713_All	6.5	14.3	Formamidase	formamidase [Osjg]	KEGG

Vv: *Vitis vinifera*; Cl: *Canavalia lineata*; Osjg: *Oryza sativa Japonica*; Hb: *Hevea brasiliensis*; Eu: *Elaeagnus umbellata*; Np: *Nicotianaplum baginifolia*; At: *Arabidopsis thaliana*; Ac: *Actinidia chinensis*; Cc: *Coffea canephora*; Me: *Manihot esculenta*; Ib: *Ipomoea batatas*; Sp: *Securigera parviflora*; Ha: *Helianthus annuus*; Pt: *Populus trichocarpa*; Gm: *Glycine max*; Lt: *Liriodendron tulipifera*; Mt: *Medicago truncatula*; Nt: *Nicotiana tabacum*; Alsl: *Arabidopsis lyrata* ssp. *lyrata*; Vf: *Vernicia fordii*; Zm: *Zea mays*.

plants. It was reported that GS over-expression can improve the efficiency of nitrogen use and promote plant growth[33]. In addition, the GDH pathway supplements the GS/GOGAT cycle for ammonia assimilation. GDH has a dual function, as it can catalyze ammonia assimilation and help glutamate oxidative deamination[34]. Under conditions of excess ammonia, GDH deamination is markedly increased in plants, providing a carbon skeleton for the citric acid cycle[35]. Both GS and GDH play an important role in maintaining balance between carbon and nitrogen (C/N) in metabolic processes[36]. The results of our transcriptomics analysis showed that expression levels of GS and GDH were higher in *I. cairica* than those in other two related species, indicating that invasive *I. cairica* may have a stronger ability to assimilate ammonia in plants.

Asparagine synthetase (AS) catalyzes the synthesis of asparagine from inorganic amine, which is the main form of organic nitrogen for transport and storage. It is involved in primary and secondary metabolism, signal transduction pathways, metabolic stress, aging, and other physiological and biochemical processes[37]. Additionally, *AS* overexpression in plants increases the level of free asparagine and promotes plant growth[38]. We found that the invasive plant *I. cairica* showed up-regulated expression of *AS* gene compared with the related species, which would favor the transportation and storage of organic nitrogen in *I. cairica*.

Phenylalanine ammonia-lyase (PAL) is a key enzyme conducting the transition from primary to secondary metabolism in plants. PAL catalyzes deamination of L-phenylalanine into cinnamic acid. This process is the central step in the secondary metabolic pathway. PAL, the first enzyme in the phenyl acid metabolic process, is deemed the first key enzyme[39]. PAL plays an important role in pigment formation, cell differentiation and lignification processes, resistance to diseases, conditions of pest and adversity, and other processes[40]. PAL catalyzes amino acids into nitrogen compounds, which provides more nitrogen resources for other metabolites in plants. Our transcriptomics analysis showed that the gene coding for PAL had a higher expression level in *I. cairica* than in the two related species, and this higher expression may lead to the enhancement of nitrogen catalytic efficiency in nitrogen metabolism.

L-ascorbate oxidase (AO) is a copper-containing oxidase, mainly located in the cytoplasm or cell wall, which can catalyze the oxidation of ascorbic acid. AO regulates stress response, gene expression, growth and development, and floral induction in plants[41]. Our transcriptomics data suggested that some of the unigenes modulating AO were up-regulated while others were down-regulated in *I. cairica* compared with those in the two related species. These levels may adapt with the function of AO, which requires further study.

The remaining genes related to plant growth and development, resource utilization, and resistance encode monooxygenases, carbonic anhydrase, cyanate lyase and formamidase. Dimethylaniline monooxygenase is the most important monooxygenase system. Carbonic anhydrase activity is positively correlated with the net photosynthetic rate in *Brassica campestris* and is very important for adapting to different nitrogen environments[42]. Under conditions of nitrogen deprivation, the gene that codes for formamidase will up-regulate to adapt to the environment[43].

Thus, overall, the DEGs involved in the nitrogen metabolism pathway may provide some clues and references from different aspects to understand nitrogen utilization in *I. cairica*.

2.11 Secondary metabolism

PAL exists in all higher plants. It is encoded by multigene families, and its genetic traits are conserved. A previous study constructed a molecular evolutionary tree using Clustalx by analyzing the bioinformatics of PAL, and plants in the same families were clustered[45]. Plants with a close kinship were also clustered[44]. The Clustalx results offered valuable information about the three plants used in the present study, which are in the same family and genus. Disease- and stress-resistance characteristics are hereditary, formed by mutual adaptation between plants and pathogenic microorganisms during evolution. Plants may undergo a series of physiological changes and defense reactions under stress, including synthesis and accumulation of disease-resistant substances such as lignin[45]. Phenylpropanoid biosynthesis is also closely related to disease resistance, and the activity of PAL is related to cold tolerance in banana plants[46]. *I. cairica* is less sensitive to cold temperatures than the non-invasive or mildly invasive plants *I. triloba* and *I. nil*, and this modification likely contributes to its ecological adaptability and invasiveness[47]. PAL plays an important role in the biosynthesis of phytoalexin and lignin as well as with other key enzymes, such as 4-coumarate, coenzyme A Ligase (4CL) and cinnamyl-alcohol dehydrogenase (CAD), all of which show highly coordinated expression. Lignin is the main component in the plant secondary cell wall[48], increasing the mechanical strength and

forming a hydrophobic network structure in the cell wall to closely link the cellulose and prevent cell wall dehydration[49]. Thus, lignin is advantageous for transporting moisture through tissues and providing resistance to adverse environments.

The expression of chalcone synthase (CHS), an enzyme in flavonoid biosynthesis (KO00944), is up-regulated in *I. cairica* compared with that in *I. digitata* and *I. nil*. The expression of another key enzyme in *I. cairica*, chalcone isomerase (CHI), is up-regulated compared with that in *I. digitata* but down-regulated compared with that in *I. nil*. The expression of a key enzyme in the metabolic pathway of flavones and flavonols, quercetin-3-*O*-*trans*-methylase, is up-regulated in *I. cairica* compared with that in both *I. digitata* and *I. nil*. Interestingly, 3-3′-5-trihydroxy-4′-7-dimethoxyflavone and 3-3′-5-trihydroxy-4′-7-dimethoxyflavone-3-*O*-sulfateare are found in *I. cairica* are chemical weapons that may inhibit the growth of other plants[50] and, intriguingly, belong to flavonoids[51−52].

These differences in the biosynthesis of secondary metabolites among *I. cairica* and other plants in the same genus may partly explain the invasiveness of *I. cairica* and the non-invasiveness of the other plants. These secondary metabolite differences may also provide a foundation for additional studies examining the stress resistance in and allelopathic effects of *I. cairica*. In addition, the results from our bioinformatics study examining the transcriptomics of *pal*, *4cl*, *cad*, *chs*, and *chi* indicate that further studies on these enzymes are warranted in *I. cairica*.

3 Conclusion

As the results suggested that the transcriptome quality obtained was good and the control samples were effective. We analyzed the biological functions and metabolic pathways associated with some of these genes. An analysis of the biosynthesis of the secondary metabolites suggested capabilities for resistance to stress, efficient reproduction, rapid growth, and allelopathy in *I. cairica* that may partly explain the invasiveness of *I. cairica* in southern China, although the complex processes of a plant invading a new region likely includes multiple genes and pathways.

As previously mentioned, the effective components of *I. cairica* have been used as folk medicine. Whereas the extracted essential oil shows larvicidal activity, arctigenin, trachelogenin, petunia-A, muricatin-B, and pinoresinol[53] provide antiviral, purgative, anti-rheumatism, and antibacterial therapies. A crude leaf extract of *I. cairica* was also shown to have oviposition-deterring activity and oviciding potential against dengue vectors[54]. Interestingly, these effective components are mainly products of secondary metabolism, indicating that studies on the biosynthesis of secondary metabolites may reveal an economic value for *I. cairica*. Thus, even though *I. cairica* is an invasive weed, it may also serve as a valuable resource, providing effective medicinal compounds.

Acknowledgments We thank the Beijing Genomics Institute at Shenzhen (BGI) for assisting in sequencing, and associate professor Jing Li from Shanghai Jiao Tong University for offering valuable suggestions regarding the bioinformatics analyses.

Refferences

[1] GONG N, WANG Y T, BJÖRN L O, et al. DNA C-value of 20 invasive alien species and 3 native species in South China [J]. Arch Biol Sci, 2014, 66(4): 1465–1472. doi: 10.2298/ABS1404465G.

[2] LI W H, TIAN X S, LUO J N, et al. Effects of simulated defoliation on growth and photosynthetic characteristics of an invasive liana, *Ipomoea cairica* (Convolvulaceae) [J]. Invas Plant Sci Managem, 2012, 5(2): 282– 289. doi: 10.1614/IPSM-D-11-00088.1.

[3] LI W H, LUO J N, TIAN X S, et al. Patterns of defoliation and their effect on the plant growth and photosynthetic characteristics of *Ipomoea cairica* [J]. Weed Biol Manage, 2012, 12(1): 40–46. doi: 10.1111/j.1445-6664.2012.00432.x.

[4] WANG R L, ZENG R S, PENG S L, et al. Elevated temperature may accelerate invasive expansion of the liana plant *Ipomoea cairica* [J]. Weed Res, 2011, 51(6): 574–580. doi: 10.1111/j.1365-3180.2011.00884.x.

[5] THOMAS T G, RAO S, LAI S. Mosquito larvicidal properties of essential oil of an indigenous plant, *Ipomoea cairica* Linn. [J]. Jpn J Infect Dis, 2004, 57(4): 176–177.

[6] THIAGALETCHUMI M, ZUHARAH W F, RAMI R A, et al. Assess-

ment of residual bio-efficacy and persistence of *Ipomoea cairica* plant extract against *Culex quinquefasciatus* Say mosquito [J]. Trop Biomed, 2014, 31(3): 466–476.

[7] LIN R J, CHEN C Y, LO W L. Cytotoxic activity of *Ipomoea cairica* [J]. Nat Prod Res, 2008, 22(9): 747–753. doi: 10.1080/14786410701628739.

[8] LIN Z F, CHEN L H, ZHANG W Q. Peroxidase from *Ipomoea cairica* (L.) SW. isolation, purification and some properties [J]. Proc Biochem, 1996, 31(5): 443–448. doi: 10.1016/0032-9592(95)00088-7.

[9] SHEKHAR S, MISHRA D, BURAGOHAIN A K, et al. Comparative analysis of phytochemicals and nutrient availability in two contrasting cultivars of sweet potato (*Ipomoea batatas* L.) [J]. Food Chem, 2015, 173: 957–965. doi: 10.1016/j.foodchem.2014.09.172.

[10] LI R, YU C, LI Y, et al. SOAP2: An improved ultrafast tool for short read alignment [J]. Bioinformatics, 2009, 25(15): 1966–1967. doi: 10.1093/bioinformatics/btp336.

[11] ISELI C, JONENEEL C V, BUCHER P. ESTScan: A program for detecting, evaluating, and reconstructing potential coding regions in EST sequences [C]// Proceedings of the 7th International Conference on Intelligent Systems for Molecular Biology. California: AAAI Press, 1999: 138–158.

[12] PERTEA G, HUANG X Q, LIANG F, et al. *TIGR* gene indices clustering tools (TGICL): A software system for fast clustering of large EST datasets [J]. Bioinformatics, 2003, 19(5): 651–652. doi: 10.1093/bioinformatics/btg034.

[13] KANEHISA M, ARAKI M, GOTO S, et al. KEGG for linking genomes to life and the environment [J]. Nucl Acids Res, 2008, 36: D480–D484. doi: 10.1093/nar/gkm882.,

[14] AUDIC S, CLAVERIE J M. The significance of digital gene expression profiles [J]. Genome Res, 1997, 7(10): 986–995. doi: 10.1101/gr.7.10.986.

[15] BENJAMINI Y, YEKUTIELI D. False discovery rate: Adjusted multiple confidence intervals for selected parameters [J]. J Amer Statist Assoc, 2005, 100(469): 71–81. doi: 10.1198/016214504000001907.

[16] MORTAZAVI A, WILLIAMS B A, McCUE K, et al. Mapping and quantifying mammalian transcriptomes by RNA-Seq [J]. Nat Methods, 2008, 5(7): 621–628. doi: 10.1038/nmeth.1226.

[17] CONESA A, GÖTZ S, GARCÍA-GÓMEZ J M, et al. Blast2GO: A universal tool for annotation, visualization and analysis in functional genomics research [J]. Bioinformatics, 2005, 21(18): 3674–3676. doi: 10. 093/bioinformatics/bti610.

[18] PFAFFL M W. A new mathematical model for relative quatification in real-time RT-PCR [J]. Nucl Acids Res, 2001, 29(9): e45. doi: 10.1093/nar/29.9.e45.

[19] LU R K. Chemical Analysis of Soil Agriculture [M]. Beijing: China Agricultural Science and Technology Press, 2000: 308–311. (in Chinese)

[20] HAO J J, KANG Z L, YU Y. Plant Physiology Experimental Techniques [M]. Beijing: Chemical Industry Press, 2007: 62–64. (in Chinese)

[21] ZUO Y M, LIU Y X, ZHANG F S. Effects of improved iron nutrition of peanut intercropped with maize on carbon and nitrogen metabolism and nitrogen-fixing of peanut nodul [J]. Acta Ecol Sin, 2004, 24(11): 2584–2590. doi: 10.3321/j.issn:1000−0933.2004.11.034. (in Chinese)

[22] GUO Z L, SHEN A L, KOU C L, et al. The relationship between NRA and nitrogen efficiency of different wheat varieties after flowering [J]. Chin Agri Sci Bull, 2008, 24(5): 219–223. (in Chinese)

[23] BESSON-BARD A, GRAVOT A, RICHAUD P, et al. Nitric oxide contributes to cadmium toxicity in Arabidopsis thaliana by promoting cadmium accumulation in roots and by up-regulating genes related to iron uptake [J]. Plant Physiol, 2009, 149(3): 1302–1315. doi: 10.1104/pp.108.133348.

[24] BECKER T W, CARRAYOL E, HIREL B. Glutamine synthetase and glutamate dehydrogenase isoforms in maize leaves: Localization, relative proportion and their role in ammonium assimilation or nitrogen transport [J]. Planta, 2000, 211(6): 800–806. doi: 10.1007/s004250000355.

[25] NORTON J B, MONACO T A, NORTON U. Mediterranean annual grasses in western North America: Kids in a candy store [J]. Plant Soil, 2007, 298(1/2): 1–5. doi: 10.1007/s11104-007-9364-8.

[26] ELBERSE I A M, van DAMME J M M, van TIENDEREN P H. Plasticity of growth characteristics in wild barley (*Hordeum spontaneum*) in response to nutrient limitation [J]. J Ecol, 2003, 91(3): 371– 382. doi: 10.1046/j.1365-2745.2003.00776.x.

[27] LI W H, ZHANG C B, LIN J Y, et al. Characteristics of nitrogen metabolism and soil nitrogen of invasive plants [J]. J Trop Subtrop Bot, 2008, 16(4): 321–327.

[28] MEYER C, STITT M. Nitrate reduction and signaling [M]// LEA P J, MOROT-GAUDRY J-F. Plant Nitrogen. Berlin Heidelberg: Springer, 2001: 37–59. doi: 10.1007/978-3-662-04064-5_2.

[29] OLIVEIRA H C, JUSTINO G C, SODEK L, et al. Amino acid recovery does not prevent susceptibility to *Pseudomonas syringae* in nitrate reductase double-deficient *Arabidopsis thaliana* plants [J]. Plant Sci, 2009, 176(1): 105–111. doi: 10.1016/j.plantsci.2008.09.017.

[30] DIAO Z W, YU X, WANG Y B, et al. Study on nitrate reductase and nitrite reductase coupled regulation of sugar beet [J]. J Nucl Agri Sci, 2014, 28(1): 138–145. doi: 10.11869/j.issn.1000−8551.2014. 01.0138.

(in Chinese)

[31] KYAING M S, GU L J, CHENG H M. The role of nitrate reductase and nitrite reductase in plant [J]. Curr Biotechn, 2011, 1(3): 159–164.

[32] MIFLIN B J, HABASH D Z. The role of glutamine synthetase and glutamate dehydrogenase in nitrogen assimilation and possibilities for improvement in the nitrogen utilization of crops [J]. J Exp Bot, 2002, 53(370): 979–987.

[33] CAI H M, ZHOU Y, XIAO J H, et al. Overexpressed glutamine synthetase gene modifies nitrogen metabolism and abiotic stress reponses in rice [J]. Plant Cell Rep, 2009, 28(3): 527–537. doi: 10.1007/s00299-008-0665-z.

[34] GULATI A, JAIWAL P K. Effect of NaCl on nitrate reductitase, glutamate dehydrogenase and glutamate in *Vigna radiata* calli [J]. Biol Plant, 1996, 38: 177–183.

[35] ROBIN S A, SLADE A P, FORE G G, et al. The role of glutamate dehydrogenase in plant nitrogen metabolism [J]. Plant Physiol, 1991, 95(2): 509–516.

[36] PACZEK V, DUBOIS F, SANGWAN R, et al. Cellular and subcellular localisation of glutamine synthetase and glutamate dehydrogenase in grapes gives new insights on the regulation of carbon and nitrogen metabolism [J]. Planta, 2002, 216(2): 245–254. doi: 10.1007/s00425-002-0854-x.

[37] GAUFIEHON L, REISDORF-CREN M, ROTHSTEIN S J, et al. Biological functions of asparagine synthetase in plants [J]. Plant Sci, 2010, 179(3): 141–153. doi: 10.1016/j.plantsci.2010.04.010.

[38] BREARS T, LIU C, KNIGHT T J, et al. Ectopic overexpression of asparagine synthetase in transgenic tobacco [J]. Plant Physiol, 1993, 103(4): 1285–1290.

[39] CAPELL T, CHRISTOU P. Progress in plant metabolic engineering [J]. Curr Opin Biotechn, 2004, 15(2): 148–154. doi: 10.1016/j.copbio.2004.01.009.

[40] Zhang K C, Jin Q, Can Y P, et al. Research progress of PAL and its control function of important secondary metabolites [J]. Chin Agri Sci Bull, 2008, 24(12): 59–62. (in Chinese)

[41] SANMARTIN M, DROGOUDI P A, LYONS T, et al. Over-expression of ascorbate oxidase in the apoplast of transgenic tobacco results in altered ascorbate and glutathione redox states and increased sensitivity to ozone [J]. Planta, 2003, 216(6): 918–928.

[42] XIA J R, HUANG J. Impacts of nitrogen and phosphorus on inorganic carbon utilization and carbonic anhydrase activity in *Nitzschia closterium* f. *minutissima* [J]. Acta Ecol Sin, 2010, 30(15): 4085–4092. (in Chinese)

[43] RATH M, SALAS J, PARHY B, et al. Identification of genes induced in proteoid roots of white lupin under nitrogen and phosphorus deprivation, with functional characterization of a formamidase [J]. Plant Soil, 2010, 334(1): 137–150. doi: 10.1007/s11104-010-0373-7.

[44] KHALIK K A, OSMAN G, AL-AMOUDI W. Genetic diversity and taxonomic relationships of some *Ipomoea* species based on analysis of RAPD-PCR and SDS-PAGE of seed proteins [J]. Ausr J Crop Sci, 2012, 6(6): 1088–1093.

[45] YOON V, NODWELL J R. Activating secondary metabolism with stress and chemicals [J]. J Ind Microbiol Biotechn, 2014, 41(2): 415–424. doi: 10.1007/s10295-013-1387-y.

[46] WANG Y, XIE H, ZHANG Z Q, et al. Relationship between chilling injury of banana fruit stored at low temperature and PAL activity and soluble proteins [J]. J Fruit Sci, 2004, 21(2): 149–152. doi: 10.3969/j.issn.1009−9980.2004.02.013. (in Chinese)

[47] PÁSKA C, INNOCENTI G, KUNVÁRI M, et al. Lignan production by *Ipomoea cairica* callus cultures [J]. Phytochemistry, 1999, 52(5): 879–883. doi: 10.1016/S0031-9422(99)00304-0.

[48] PICKETT J A. Genetic engineering of secondary metabolism for plant protection [J]. New Biotechn, 2014, 31(Suppl): S55. doi: 10.1016/j.nbt.2014.05.1737.

[49] THAKUR V K, THAKUR M K. Recent advances in green hydrogels from lignin: A review [J]. Int J Biol Macromol, 2015, 72: 834–847. doi: 10.1016/j.ijbiomac.2014.09.044.

[50] MA R J, WANG N L, ZHU H, et al. Isolation and identification of alleiochemicals from invasive plant *Ipomoea cairica* [J]. Allel J, 2009, 24(1): 77–84.

[51] ERREIRA A A, SILVEIRA D, ALVES R B, et al. Constituents of *Ipomoea cairica* ethanolic extract [J]. Chem Nat Comp, 2005, 41(4): 465. doi: 10.1007/s10600-005-0178-8.

[52] FERREIRA A A, AMARAL F A, DUARTE I D G, et al. Antinociceptive effect from *Ipomoea cairica* extract [J]. J Ethnopharmac, 2006, 105(1/2): 148–153. doi: 10.1016/j.jep.2005.10.012.

[53] PÁSKA C, INNOCENTI G, FERLIN M, et al. Pinoresinol from *Ipomoea cairica* callus cultures [J]. Nat Prod Lett, 2002, 16(5): 359–363.

[54] AHBIRAMI R, ZUTMA F W, YAHAYA Z S, et al. Oviposition deterring and oviciding potentials of *Ipomoea cairica* L. leaf extract against dengue vectors [J]. Trop Biomed, 2014, 31(3): 456–465.